A pressure modulator radiometer for measuring stratospheric trace gases

J. R. Drummond, D. Turner, and A. Ashton

Department of Physics, University of Toronto, Toronto, Ontario, Canada M5S 1A7

(Received 30 December 1989; accepted for publication 23 June 1989)

This article describes a pressure-modulator instrument which is designed to measure trace constituents of the stratosphere from a balloon platform at an altitude of about 40 km. Double-sided limb-scanning allows profiling below the instrument and a direct determination of the instrument attitude from the radiance data. The instrument is described in detail and the methods of radiance measurement and calibration are discussed. Some of the supporting laboratory measurements are described. A concentration profile of carbon monoxide from 20 to 45 km is presented as an example of the results of the first series of flights.

INTRODUCTION

Chemically active trace constituents of the upper atmosphere are important because the chemical balance of the region affects the radiation balance, and hence the dynamics. Therefore these compounds, although present in very small amounts, can have a significant overall effect upon the state of the stratosphere. However measurements of these compounds are hampered by their low concentrations and the small signals which they produce.

Pressure modulator radiometry is a technique by which small signals from the thermal emissions of constituents can be detected and analyzed to determine a concentration profile. Previous applications of this technique have been to temperature sounding and to constituent measurements.[1] The temperature sounding instruments, using CO_2 as the pressure modulating gas, have been flown on balloons and satellites, notably the pressure modulator radiometer (PMR) instrument on the Nimbus 6 satellite and as part of the stratospheric and mesospheric sounder (SAMS) instrument on Nimbus 7. In the area of composition measurements, previous balloon-borne instruments have measured nitrogen oxides[2,3] and a variety of measurements have been made using the SAMS instrument mentioned above.[4] The principal advantages of the technique are the large energy grasp, which serves to increase the available signal, and the high effective spectral resolution, which enables the instrument to detect signals from specific gases while rejecting those from other species. This is achieved without sensitive mechanical or optical systems, allowing the instrument to be readily used in balloon-borne and satellite systems.

This article discusses a new balloon-borne instrument which is designed as a general-purpose instrument for stratospheric composition measurements. For the first experiments the instrument, which has three independent channels, was equipped to measure carbon monoxide at 4.7 μm, methane at 7.6 μm, and formaldehyde at 5.7 μm.

I. PRESSURE MODULATION TECHNIQUES

A. Overall description

The schematic of a pressure modulator radiometer is shown in Fig. 1. It consists of a conventional filter radiometer with a fast chopper at the input to modulate the radiation and an additional cell, the pressure modulator cell or PMC, filled with the gas being studied. The density of the gas is cycled mechanically at a rate which is much less than the modulation frequency of the chopper. The fast chopper alternately selects the atmospheric signal or an internal reference signal. A discussion of the spectral, mechanical, and signal characteristics of a modulator is given below with particular emphasis on features which are used in the instrumentation to be described.

B. Spectral characteristics

The essential feature of the pressure modulation technique is the use of the emission lines of the gas itself as a precise optical filter for incoming signals. Variations in the density of the gas in the modulator cell cause variations in the absorption of incoming radiation only in spectral regions near spectral lines of that gas (Fig. 2). Electronic systems can extract this signal which, being a function of radiation near spectral lines of the gas in the cell, is likely to be indicative of emission from the same gas. There is a precise correlation between the radiation coming in from the gas in the

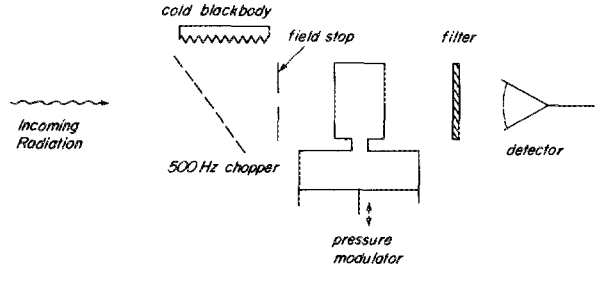

FIG. 1. Schematic of a pressure modulator radiometer. Radiation enters the system from the left-hand side and is interrupted by a fast rotating chopper. The rear face of the chopper is reflecting and therefore the ongoing radiation in the system is alternately the input radiation and the radiation from the reference blackbody. The field of view is delineated by the field stop. The radiation then passes through the pressure modulator cell containing a sample of the gas being measured. The gas density is varied cyclically at about 11 Hz. The radiation is spectrally limited by a conventional multilayer filter and then falls on a detector. The signal produced is processed by the electronics to produce "wideband" and "sideband" signals.

 0034-6748/89/113522-11$01.30

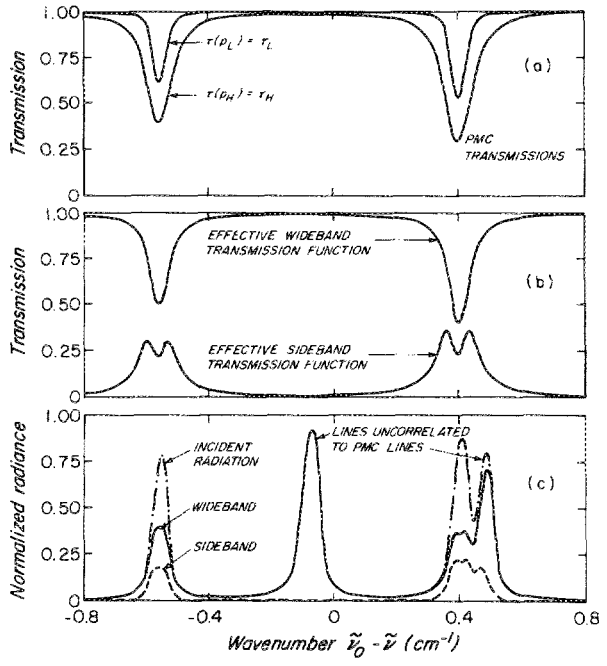

FIG. 2. The operation of the pressure modulator cell in spectral space. Figure (a) shows the transmission function of the modulator gas in spectral space at its two pressure extremes. The effect of the PMC in a PMR, after electronic processing, is the replacement of a single gas cell/detector channel by two independent channels, each containing an effective transmission filter (b) instead of a gas cell. One of these filters has an effective transmission function equal to the average transmission function of the two transmission extremes, the other to the transmission differences. The resulting detected radiances (c), are known as the "wideband" and the "sideband" response, respectively. The PMR output is the total detected radiant energy integrated over wave-number space from each channel.

atmosphere and the absorption features of the same gas in the cell. Since this perfect spectral alignment is achieved without any dispersing components and their attendant adjustments, the instrument is inherently robust.

The selection of the spectral region to be used is determined by the constraints of maximum signal and minimum contamination of that signal by emission from other gases resulting from chance coincidences between the spectral lines of the required and contaminant gas. Since any specific gas being studied has only a few infrared vibration-rotation bands, the choice is often not perfect and it will be necessary to account for some contaminant signal.

Chance co-incidences between spectral lines of the desired gas and other gases, particularly of plentiful constituents such as water, do occur as shown in Fig. 2(c). These must be allowed for by exact calculation requiring knowledge of the concentration profile of the contaminant. Since it is desirable to obtain this profile as accurately as possible, the "wideband" signal is used as an additional source of information. This signal is the total signal received, attenuated by a cell transmission function appropriate to an average cell pressure. It may be obtained simultaneously with the pressure modulator signal by methods discussed below. This overall signal is usually influenced more by the contaminant gas(es) than the gas under observation. Thus, for a CO modulator the wideband signal is almost entirely due to ozone whereas the pressure modulator signal is 70% due to O_3, 30% due to CO. In this case an ozone profile can be determined first using the wideband signal and then that profile used to calculate the effect on the pressure modulator signal.

C. Signal calibration

The reference signal (Fig. 1), which is viewed alternately with the atmosphere, must be very stable. If it is not stable then it is very difficult to separate out the effects of a variable reference from those of the atmosphere. In order to achieve such stability, a separate blackbody source and a reflecting chopper is used, rather than the emission of the chopper blade alone. The two choices for the reference blackbody temperature are room temperature, which is easy to manufacture, or a low-temperature source, which produces almost zero radiation. The choice of a cold blackbody is appropriate for an atmospheric emission sensor as this signal is comparable with the small atmospheric signal. The use of a room temperature source would mean that the two signals were always significantly different and comparatively small relative variations in the large reference signal would become important.

D. Mechanical characteristics

Since the oscillation in gas pressure is essential to the operation of the instrument, care must be taken to maximize this without compromising other parameters. Typically compression ratios of 3:1 are used in the cells at oscillation frequencies in the range 10–20 Hz. The frequency used is a compromise between a low frequency which simplifies the mechanics, and a high frequency which is easier to deal with in the electronics and leads to fewer problems with gas leakage. Previous instruments have used various designs for the cell, most of which have required extreme care in fabrication and assembly.[1] Our new design, described in Sec. III B, is simple to assemble but requires more drive power.

It is evident that a modulator running at a sufficiently low frequency will have isothermal compression cycles, whereas one running at a high frequency will have adiabatic compression cycles. In general, modulators run somewhere between these two extremes and although we have some evidence for temperature cycling in our modulators, it appears from measurements that the cycle is predominantly isothermal.[5]

E. Signal characteristics

Incoming radiation is modulated first by the chopper and then by the modulator. The pressure modulator signal therefore appears both as a "baseband" signal at the modulator frequency and as sidebands around the chopper frequency ($\sim$500 Hz). The sideband signal is the one processed by the electronics for two reasons: First, the increase in frequency from the basic modulator rate to almost the chopper frequency, improves the signal-to-noise ratio obtainable with many detectors as it raises the frequency above that of significant $1/f$ noise. Second, thermal emissions from the modulator, modulator gas and the associated optics, which are either approximately constant or vary at the modulator frequency, are easily filtered out in the electronics.

If the volume of an isothermal pressure modulator is varied sinusoidally at a frequency f, then the density variation is given by

$$1/[1 + A \sin(2\pi ft)],$$

where the constant A is related to the compression ratio, U, by $A = (U - 1)/(U + 1)$. Since the density modulation is not sinusoidal, the signal modulation will not be sinusoidal and there will be sidebands at harmonics of the PMC frequency about the chopper frequency. In the case of a rotating high-frequency chopper, there will also be sidebands due to the imperfections of the blade which occur at harmonics of the chopper rotation rate. All these effects can clearly be seen in Fig. 3 which illustrates the complexity of the modulated signal after detection. The electronics necessary to extract the sideband signal are described in Sec. III C.

II. LIMB-SCANNING

The technique of "limb-scanning" is used to maximize the amount of material within the field-of-view or the balloon-borne instrument. The atmosphere is viewed almost horizontally as shown in Fig. 4. The amount of material in a limb path is up to 70× that in a corresponding vertical path with the same lowest height, known as the "tangent height." In the case of an absorber with a constant mixing ratio at all altitudes, the signal from a limb path is strongly weighted by the atmospheric pressure profile to the tangent height producing a narrow weighting function[6] and therefore good vertical resolution. Different regions of the atmosphere are sampled by varying the view angle in a step-wise manner during an instrument "scan." An additional advantage is that the background to any limb path is space which is effectively a zero signal source for an infrared instrument.

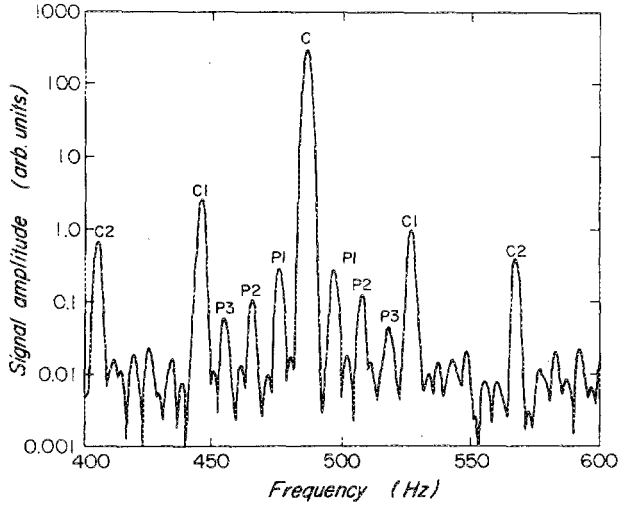

FIG. 3. A spectral analysis of the electronic signal produced from the detector in Fig. 1 for the particular case of a CO pressure modulator. The region of the spectrum around the chopper frequency is shown. The central peak (C) is the chopper fundamental. The average value of this signal is the "wideband" component. The pressure modulator sidebands (marked P1, P2, and P3) can be seen and the average magnitude of these represents the "sideband" signal. The peaks marked C1 and C2, are the subharmonics of the chopper due to the imperfections of the 12-bladed system. These occur at about 41-Hz intervals.

The major disadvantages of limb-scanning are the poor horizontal resolution, the complexity of the path and the necessity of knowing the view angle very precisely.

This last problem of determining the tangent height of the view is critical to correct retrieval of the concentration profile. In order to determine the tangent height to an accuracy of $\pm$ 0.5 km at 15 km from a balloon at 40 km, the angle must be known to within $\pm$ 0.05°. This angle is measured relative to the horizontal, which is taken as the tangent to the average isobaric surfaces in the stratosphere.

We measure the angle of the optical beam relative to the horizontal by using the information contained in double-sided scanning data which is shown in Fig. 4. The direction of view of the instrument is steered by a single mirror (see below) which is capable of rotation through nearly a full circle.

Since a scan position obtained using the shaft encoder is measured relative to the package, the package must be stable during a complete scan sequence ($\sim$ 10 min) in order to be able to compare the two sets of data. Within this constraint, any differences between left and right scans are attributed to instrumental effects, which may be the tilt of the package or asymmetry of the beam under rotation. The latter occurs if the optics are not truly axial and can be successfully eliminated by careful alignment.

We define α as the dip angle of the beam between the nominal horizontal and the true horizontal, and the beam asymmetry angle, β, as the excess angle by which the beam rotates when the mirror is rotated by exactly 180°.

If we select a case when the left and right signals are identical, then if the atmosphere is horizontally homogeneous, the true depression angles for the two cases are identical. If the true angle is θ and the measured angles for these cases are L and R, we find (Fig. 5) that

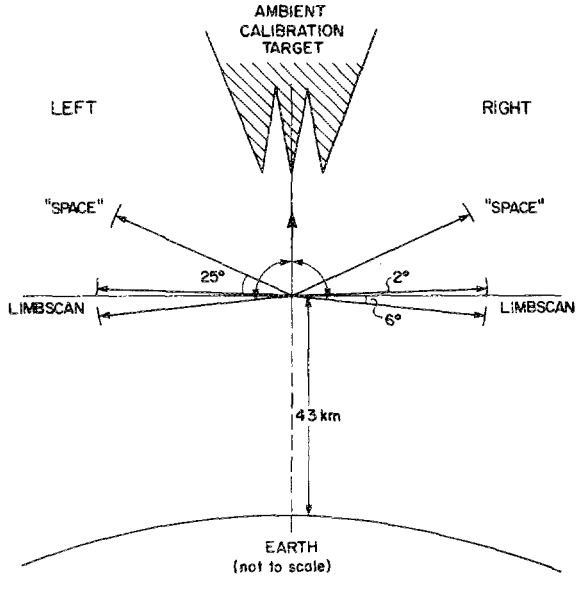

FIG. 4. Schematic of the TORBAR implementation of limb scanning. The atmosphere is viewed from two sides of the instrument by scanning at angles between $-2°$ and 6° from the local horizontal. A radiation "zero" is established by views at $-25°$ and a known radiance by rotating to $-90°$ to view an internal calibration target of known emissivity and temperature.

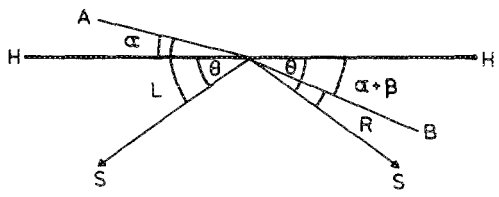

FIG. 5. Scanning geometry. H-H is the true horizontal and the lines A and B are the beam orientations when the shaft encoder indicates horizontal. The error comprises two parts: The dip angle α which is a measure of the package tilt, and the beam asymmetry angle β which is the angular error in the beam between the two "horizontal" positions. The apparent angles L and R are the results of measurements at the true angle θ at which the left and right signals are equal. These measurements are affected by the dip angle and beam asymmetry angle, resulting in the equations for the apparent angles $L = \theta + \alpha$ and $R = \theta - \alpha - \beta$.

$$L = \theta + \alpha$$

and

$$R = \theta - \alpha - \beta$$

or

$$L - R = 2\alpha + \beta = \gamma,$$

where γ is defined as the tilt angle.

By comparing left and right scans using a least squares technique for each scan we can determine α and β, and then using estimates from scan pairs throughout the flight, we can then estimate γ as a function of time.

The ideal signal source for this measurement is one which is large, shows a strong dependence on scan angle and is uniform in space and time. The wideband signals fulfill these requirements, being predominantly due to the more plentiful minor constituents such as water and carbon dioxide. We use the wideband signal from the formaldehyde channel centered at 1746 cm^{-1} for our attitude sensing, whose signal is predominantly due to water.

Using scan pairs throughout the flight, we can estimate γ as a function of time. Data from the area of the tropopause are eliminated and the various estimates in the scan weighted appropriately. The function

$$\sum_j [S_L(k_j) - S_R(k_j + \gamma)]^2$$

is minimized, where S is the signal, k the nominal scan angle, subscripts L and R refer to left and right scans, respectively. The sum is done over a restricted range of scan positions, interpolating data between real data points using a linear formula. The sum of squared residuals is shown in Fig. 6 as a function of the angle γ and a definite minimum is found. A more complete discussion of this technique has been given in a previous paper.[7]

A limb-scanning instrument is generally only able to derive concentration profiles from flight altitude down. For view angles above the balloon the material in the path is weighted towards the balloon level for all scan angles and therefore vertical resolution is poor. For view angles below the balloon the path between the tangent height and the balloon becomes less transparent at wavelengths where the instrument is sensitive and eventually becomes opaque as the tangent height moves down through the atmosphere. When the path becomes opaque before the tangent height is reached, the instrument does not detect emission from the tangent level and the concentration profile is again indeterminate. The level at which the instrument loses sensitivity can be adjusted to a certain extent by adjusting the pressure in the pressure modulator cell, but as sensitivity to lower levels is increased, sensitivity to upper levels is decreased.

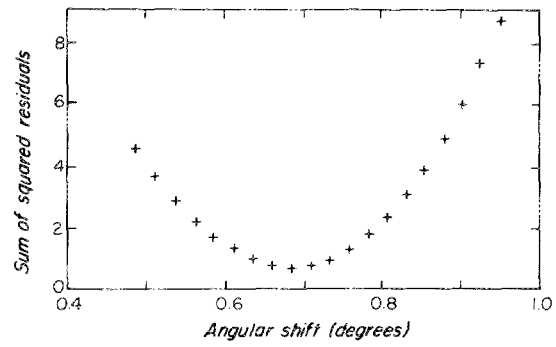

FIG. 6. Sum of squared residuals for some flight data (from the flight of August 1983) as a function of γ. The vertical scale is in units of [nW m^{-2} sr^{-1} (cm^{-1})]^2. A definite minimum can be seen at 0.68°. Data from views near the tropopause are excluded from the summation as these are not expected to be similar for the two scans.

III. THE TORONTO BALLOON RADIOMETER (TORBAR)

A. Optical design

The Toronto Balloon Radiometer is a three-channel instrument designed to sense thermal emission using double-sided limb scanning. The optical design is shown in Fig. 7. It consists of a scanning mirror, M1, a simple 0.1-m-diam telescope and folding optics, M2/3/4, a field lens and field splitter assembly, L1/M6a/M6b, followed by an individual PMC for each channel and detector optics discussed below. Since the energy available is small, care must be taken to maximize the energy usage of the instrument consistent with its size and other constraints. This can be at the expense of image quality if the field-of-view can be maintained. A ray-trace computer program was used to aid the design and the final result has efficient energy collection but relatively poor image quality. Compromises had to be made, particularly in the area of the field lens, L1, as many components need to be situated at the field stop position for maximum efficiency. The optics is not spectrally selective as gold coatings are used for all the mirrors and calcium fluoride for the field lens and all windows in the individual channels.

An important feature of the instrument is the facility for two-sided limb scanning discussed above. This is realized by the 45° scanning mirror M1 which is pivoted on an axis aligned with the optical axis of the system. The mirror can rotate through almost 360° and therefore input radiation can come from either side of the instrument. The external instrument field of view is clear to a scan angle of $-25°$ to allow for a "space view" (see below) and at $-90°$ (vertically upwards) a reentrant cone in the instrument allows the system to view a known radiance. These last two facilities form a

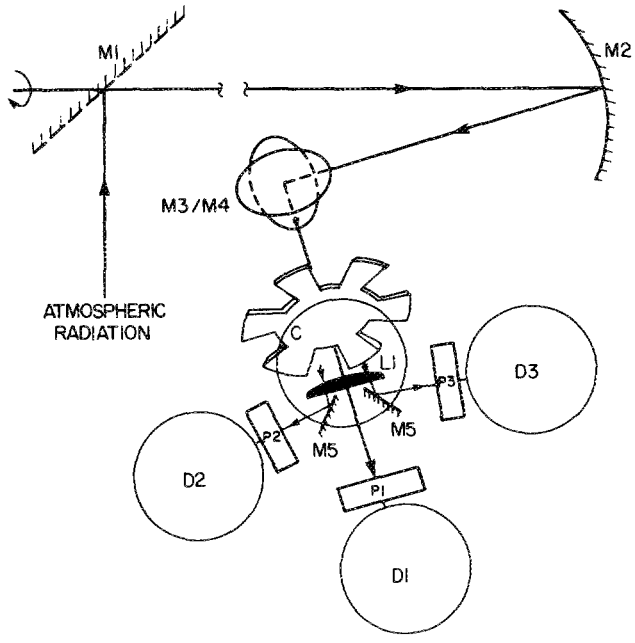

FIG. 7. Schematic (not to scale) of the main optical system of the Toronto Balloon Radiometer. Input radiation falls on M1, the scanning mirror and is then focused by M2 onto the field assembly L1/M5. Folding mirrors, M3/M4, rotate and steer the beam through the reflecting chopper C. From the field-splitting assembly, radiation passes into one of the three independent pressure modulator/detector channels (P1-P3, D1-D3) for measurement.

major part of the radiometric calibration of the system and, since they are situated at the input of the instrument, allow the emissions of the individual optical components to be eliminated from the signals. The mirror is driven by a stepper motor geared down to give a rotation of 0.163°/step. The position of the mirror is monitored independently by a shaft encoder with 0.044° resolution.

The fast rotating chopper described in Sec. III B is situated in front of L1. It is a 6-mm-thick disk of stainless steel 0.2 m in diameter with 12 blades and rotates at about 4000 r.p.m. One face of the chopper is polished and gold-plated and the instrument alternately views the atmosphere in the clear sections and a cold blackbody in the reflecting sections. The cold blackbody is cooled with liquid nitrogen and is contained within a dewar assembly.

The three fields-of-view of the instrument are spatially separated by the mirror pair M5a/b, the central field being undeflected. Each of the mirrors M5a, M5b can be independently adjusted for alignment purposes. The fields are delineated with a field stop on the back of L1. This is a grid or three 22 mm $\times$5 mm slots corresponding to the three fields of 2.04° horizontal $\times$0.45° vertical.

The pressure modulator optics for each channel simply consists of a pair of calcium fluoride windows for entrance and exit to the cell.

The filter, detector optics and detector for each channel are all contained within a dewar and are cooled to liquid nitrogen temperature. This has the dual advantage of decreasing the total radiation on the detector, which improves its performance in some cases, and of providing mechanical protection for these components which are the most delicate in the system. The filters are coated germanium with specific passbands for each gas. They were designed and supplied by Dr. J. Seeley of Reading University and are temperature invariant between room temperature and the cryogenic temperature of operation. The detector lens consists of an antireflection coated germanium doublet.[8] The use of a high refractive index material allows the construction of a fast, aberration-free condensing lens. The detectors used are photo-conductive, mercury-cadmium-telluride for the methane and formaldehyde channels and a photo-voltaic indium antimonide for the carbon monoxide channel.

There are a large number of sources of mechanical vibration in the instrument and therefore the detector dewars are designed to be mechanically stable with respect to the main optical plate, which is the optical reference for all the other optical components. This is achieved by anchoring the base of the cryogen vessel to the dewar base, which is in turn bolted directly on to the plate, with three short (80 mm) glass/epoxy pillars as shown in Fig. 8. The use of glass/epoxy maintains the necessary thermal isolation whilst providing the required mechanical rigidity. The fill and vent tube for the cryogen also pass through the baseplate and therefore it is necessary to fill the dewars by means of a pressurized system. Many layers of aluminized mylar are used as radiation shields and a container of molecular sieve material is attached to the cryogen vessel to adsorb as much residual

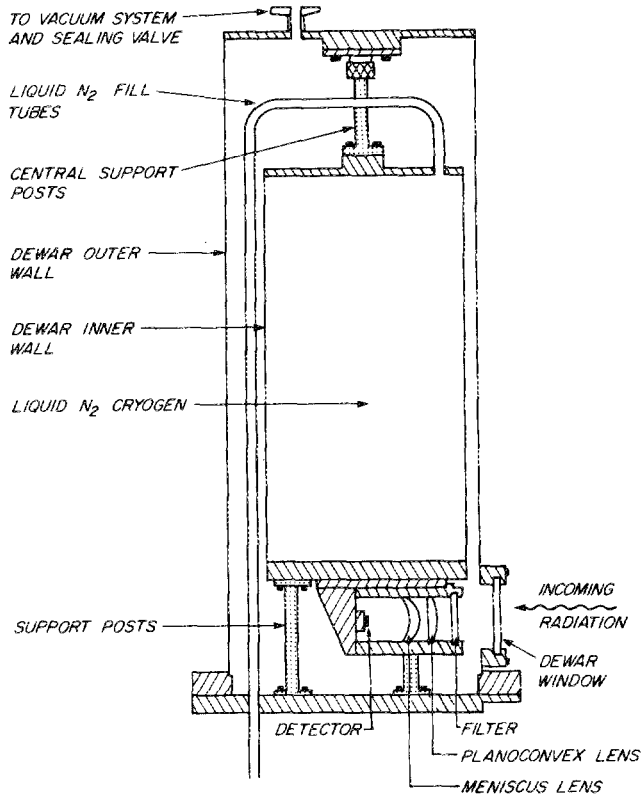

FIG. 8. Liquid nitrogen dewar (capacity of 1 ℓ) used to cool the detector optics attached to the base of the cryogen vessel. Efficient evacuation of the dewar along with multiple layers of aluminized mylar wrapped around the cryogen vessel give a cryogen lifetime of up to 40 hours. The support posts provide thermal insulation and mechanical rigidity with respect to the rest of the optical system.

gas as possible. Together with efficient evacuation of the system, these precautions reduce the heat leakage to such an extent that a duration of 24–40 h is obtained from the 1-ℓ charge of liquid nitrogen. The nitrogen vapour over the liquid is pressurized to about 10^5 Pa using an absolute pressure relief valve. This prevents excessive boil-off during balloon ascent and freezing of the liquid, with the associated loss of thermal contact between the dewar body and the cryogen, at ceiling.

Since all the frequency-selective optics are contained in the detector dewar, a change of instrument operation from one gas to another requires only the substitution of an appropriate set of detector optics and detector. This design flexibility should enable the instrument to be used for monitoring of many trace constituents in the future.

B. Pressure modulator cells

Previous designs of pressure modulator cells have used a freely suspended piston/spring arrangement driven magnetically at the resonant frequency. The gap between the piston and the bore is not sealed and gas leakage is minimized by the small size of the gap.[1] However this makes the cells difficult to manufacture and assemble. We have used a more conventional arrangement of piston and cylinder with sliding bearings and a PTFE sealing ring (Fig. 9). The drive power must be increased to compensate for the frictional losses in this arrangement but any oscillation frequency may be used as the system is nonresonant. A Ferrofluidic seal (trademark of the ferrofluidic Corporation Inc.) transmits the motor drive power through the wall of the pressure modulator cell and a flywheel/con-rod system transmits the drive to the piston. The d.c. motor consumes about six watts of power whilst running the modulator at about 11 Hz.

The pressure cycling within the modulator is monitored by a variable-reluctance diaphragm pressure sensor attached directly to the cell. The upper- and lower-pressure values are logged by the data system and the pressure cycle is used to derive a square-wave reference signal for the signal processing electronics (see below).

The formaldehyde modulator is unique in this instrument in that the gas is unstable and polymerizes in the cell. In order to maintain a constant pressure of formaldehyde, it is necessary to generate fresh gas continually. This is achieved by heating paraformaldehyde powder in a small container attached to the modulator. Paraformaldehyde decomposes into formaldehyde and water, the latter being removed by a calcium sulphate dryer. The heater is controlled by the on-board computer which maintains a constant pressure in the modulator cell using the pressure sensor described above.

C. Signal channels

As can be seen from Fig. 3, the electronic signal from the detector is very complex in nature. It is also very small. A battery-powered pre-amplifier attached to each detector raises the signal level and the signal is passed to the signal processing electronics, which are also powered by separate batteries. The use of separate power supplies minimizes ground loops and noise coupling in the system. The signal-processor is coupled to the on-board computer through opto-isolators to maintain the electrical isolation of each section.

The function of the signal processor electronics is to determine the pressure modulator signal and the overall "wideband" signal. After amplification and filtering to suppress d.c. offsets and low-frequency signals from the modulator, the signals are extracted in two stages. First a phase-sensitive detector (PSD) using a reference signal derived from the rotating chopper shifts the wideband component at the chopper frequency to d.c. and the sidebands from the

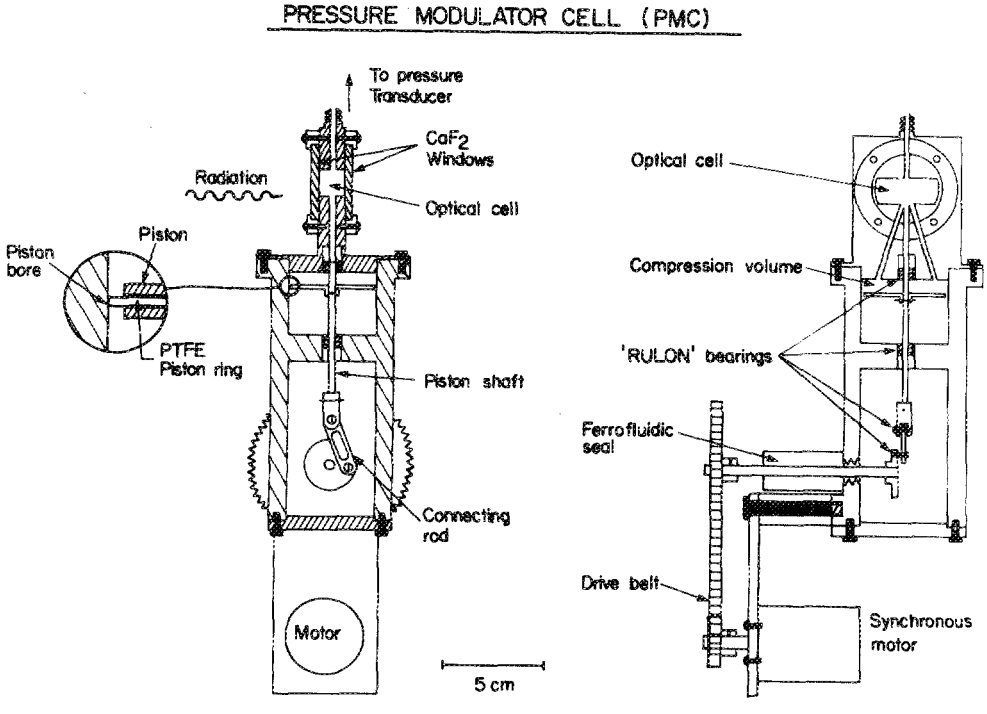

FIG. 9. Schematic of the pressure modulating cell. The optical thickness of the gas varies with the cell pressure. The pressure is varied by a piston oscillating in a cylindrical bore beneath the optical cell. The piston is driven by an internal flywheel crank and con-rod mechanism, which is connected to an external drive via a rotary vacuum seal. The system may be driven at any frequency. Pressure extremes and a square wave reference are obtained from a transducer on top of the cell. The base of the PMC may be easily modified for the inclusion of a gas source, if required (e.g., a CH_2O generator).

pressure modulator to the modulator frequency and its harmonics. The average value of this signal is the wideband output. The average signal is derived by averaging the frequency of a voltage-to-frequency converter for one second. The signal from the PSD is also applied to a filter/amplifier system tuned to the pressure modulator frequency. The passband is narrow enough to exclude the chopper sidebands (C1, C2 in Fig. 3). The resulting signal is then detected by a second phase-sensitive system using a reference derived from the modulator pressure transducer. The average value of the resulting d.c. level is obtained with a second voltage-to-frequency converter.

The voltage-to-frequency converters use a double counting system as shown in Fig. 10 to improve the overall resolution. A fast clock is counted for the nearest integer number of converter cycles that occur in one second. The average frequency is then obtained from the ratio of counts and the clock frequency. The advantage of this technique is that the average is accurate to within one cycle of the fast clock ($\sim$1 MHz), giving a theoretical resolution of 10^{-6} in one second, whereas a simple counting scheme would only be accurate to one cycle of the converter ($\sim$2 kHz). In order to ensure that the true measurement period remains approximately synchronous with the required measurement period, the converter frequency is offset from zero and is never allowed to drop to a low value. Two sets of counters are used so that measurement cycles are continuous with one set of counters being read and cleared whilst the other set is in use. The measurement cycle for each channel is also synchronized to the reference frequency of the corresponding phase-sensitive detector in order to suppress the variations in the output due to a noninteger number of reference cycles occurring in one measurement period. Synchronization ensures that there is an integer number of cycles in one measurement period and therefore cyclic variations average out exactly. This is particularly useful for the pressure modulator signal whose reference goes through only about 11 cycles in one second.

D. Overall instrument control

It was decided very early in the instrument design that the instrument should be completely computer controlled. Thus a full microcomputer system is used to control all mechanisms and measurement systems. The system also handles formatting the data frames (see Sec. V A) for transmission to the ground, producing a split-phase data stream for the data transmitters.

The command system for the instrument consists of a 16-bit word sent one bit at a time using a total of 18 commands. Sixteen of these commands set single bits in a 16-bit command word, one causes the command to be executed and one is used to reset all the bits of the command word to zero in the case of an error. The partial command word is returned in the transmitted data stream so that it can be checked before the "execute" command is sent. The commands alter the contents of the computer's operating tables which in turn determine the mode of operation of the various mechanisms. Commands are not essential for instrument operation, but are used to adjust the instrument to varying conditions, e.g., compensating for an excessive tilt by adjusting the scanning system.

There are also many temperature and other sensors in the instrument which allow the overall instrument condition to be monitored continuously. This information has been invaluable in the development phase for determining the cause of instrument anomalies and generally adjusting the performance, as well as in helping prepare the instrument for flight.

Complementary to the on-board computer system is the ground computer for real-time analysis. This takes the data stream from the instrument and decodes it in real time to produce engineering displays of the instrument status and plots of time variations. This system is also programmable to cope with various instrument conditions. The engineering display allows the continuous monitoring of over 100 parameters. The data are also recorded in several different forms for later retrieval and scientific processing.

IV. FLIGHT SUMMARY

The TORBAR instrument has been flown four times from the National Research Council of Canada facility at Gimli, Manitoba over a period of three years. The first flight in August 1983 was an engineering flight and was successful

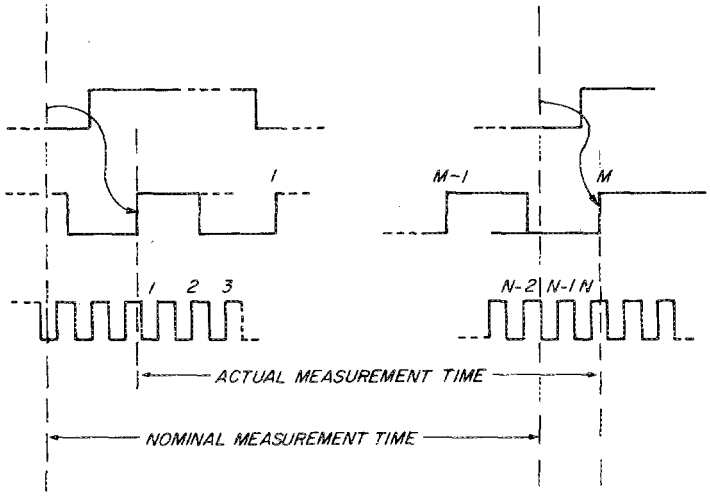

FIG. 10. The synchronization technique used for the voltage to frequency converters. A measurement period starts on the first positive edge of the reference square wave after the nominal start of the measurement period, and ends on the first positive edge after the nominal end of the period. Cyclic variations at the reference frequency therefore average out because the measurement period is an exact number of cycles in length. The measurement period is also synchronized to the output of the voltage to frequency converter. The final average frequency is $(M/N)f$, where f is the clock frequency. The resolution is $1/N$ which for a 1-MHz clock and a 1-s measurement is $\sim 10^{-6}$.

apart from landing in Lake Winnipeg which severely damaged the instrument. In 1984 the second flight was moderately successful and many of the instrument faults were corrected. In 1985 two launches were made on July 31st and August 8th. The last flight was the most successful of all. Launched on a 640 000-m^3 balloon, the instrument reached an altitude of 43.3 km with a maximum variation of 1.5 km. Data were collected for 20 h during which time all mechanisms functioned well. The instrument was successfully recovered and the post-flight checks were made without difficulty.

V. DATA PROCESSING

The data processing for the TORBAR instrument is divided into three sections. First is the reduction of the housekeeping data comprising temperature, voltage, pressure, and status readings. Second is the processing of the radiance data from the various channels to allow for instrument attitude and altitude variations and the conversion from frequency to radiance units, a process referred to as calibration. Third is the analysis of the radiance data in conjunction with other data and models to deduce concentration profiles of various gases in the atmosphere.

A. Raw data format

The data from the instrument are transmitted and stored as data frames. These occur at the rate of 1 Hz and consist of 128 16-bit words. Important quantities and/or those whose values change rapidly, e.g., radiance signals, are sampled and encoded into every frame. Quantities which generally vary more slowly are multiplexed into frame words at a slower rate. This is accomplished by three multiplexers. A fourth multiplexer slowly reads out the contents of the computer control tables for confirmation purposes. All data analysis starts from these data frames.

B. Housekeeping data

The physical quantities monitored in the instrument are easily transformed into voltages using appropriate transducers and electronics. Two instrument multiplexers measure these voltages using solid-state switches to sample the channels. The analogue-to-digital conversion scheme is a simpler version of the "double-counting" voltage-to-frequency technique used for the signal channels. Calibration voltages on some channels allow the whole multiplexer to be calibrated using a linear calibration scheme. Each individual channel can then be related to the corresponding physical quantity using a second calibration. In most cases the calibration is linear and is simply accomplished. This double calibration is performed in real time by the ground station computer so that the engineering data appears in appropriate units.

Temperatures are measured using two different techniques. Linear current sensors (National Semiconductors LM134) are used for most temperatures as the current source system is ideally suited for a large switching matrix and lead lengths are not relevant. The current multiplexer uses reed relays and diode isolation to achieve a low-leakage matrix. However the precise calibration of the sensors is difficult and it has been found that for precise, consistent temperature measurements of the blackbody and other critical components, precision thermistors (YSI Precision Thermistors 44006) whose resistance vs temperature characteristics are known to ± 0.1 °C are preferred. These are also accessed using a reed-relay switched matrix. The resistance versus temperature relationship for the thermistors is known but nonlinear and therefore a set of straight-line segments is used in the ground computer to allow the high-speed computation of the temperature. A more accurate, but more time-consuming, curve-fit scheme is employed in the final data reduction programs.

C. Signal channel data

The output from the signal channels consists of six frequencies from the corresponding voltage-frequency converters. Since the voltage-frequency and radiance-voltage relationships are both linear, a conversion directly from frequency to radiance is made. The equivalent instrument spectral passband varies somewhat as the gas pressure in the modulator drifts, and therefore it is removed from the analysis at this stage by calibrating in terms of the monochromatic blackbody signal at the center of the passband (2140, 1746, and 1308 cm^{-1} for the CO, CH_2O, and CH_4 channels, respectively) using a calibration sequence at the end of each atmosphere scan.

The instrument scans the atmosphere on each side alternately. Between the scans a view is taken at $-25°$ where the atmospheric content of the path is sufficiently small that the radiance may be taken as zero to first order. At $-90°$, as the view passes through the vertical, it is intercepted in the instrument by an ambient-temperature retro-cone blackbody of large thermal inertia. These two readings, of a zero radiance and a known Planck radiation suffice for a two-point calibration of the system. Since the accuracy of the calibration, particularly the knowledge of the zero value, is critical to the accuracy of the experiment, these views are longer than the individual atmosphere views in order to improve the signal-to-noise ratio and the zero measurement is repeated at the beginning and the end of the scan. Thus the sequence is as follows: left atmosphere–zero–blackbody–zero–right atmosphere–zero–blackbody–zero and repeat.

The calibrated measured radiances are calculated as

$$S_\alpha^\eta(\theta) = B(\tilde{\nu}_0, T_b)\,\frac{[C_\alpha^\eta(\theta) - SP_\alpha^\eta]}{(I_\alpha - SP_\alpha^\eta)},$$

where $B(\tilde{\nu}, T_b)$ is the retro-cone blackbody Planck function evaluated at its temperature and the band center of the delineating filter profile, $C_\alpha^\eta(\theta)$ is the frequency from the atmosphere view at angle θ, I_α is the frequency from the blackbody view, SP_α^η is the frequency from the $-25°$ zero view, α denotes a wideband or sideband response, and η denotes a left or right view. The values of SP_α^η, I_α, and T_b vary slowly with time and are linearly interpolated from their measurement time to the time of the atmosphere view.

Signal data are carefully checked for anomalies and noise spikes. In particular, readings taken when the mirrors are moving or stabilizing are rejected.

D. Height and attitude corrections

The initial calibrated data are not in a form that can be compared to the models. For this purpose the instrument views must be related to the atmosphere in terms of the instrument height and the view angle of the ray path or, alternatively, the tangent height. The balloon height is provided by the tracking data and the attitude of the instrument can be corrected for using the technique outlined in Sec. II. These processes result in plots of signal versus view angle which allow comparison between the experimental results and calculations using atmospheric models. A typical pair of signals (wideband and sideband) from the CO channel are shown in Fig. 11.

VI. LABORATORY TESTING

In order to verify instrument performance and the agreement of instrumental results with theoretical calculations, it is desirable to use the instrument to measure known gas concentrations in the laboratory. It is not possible to completely reproduce the atmospheric path in the laboratory since this varies in pressure, temperature, and composition along its length of up to 400 km. Laboratory experiments are restricted to measurements using a single cell of gas and a blackbody as the radiation source.

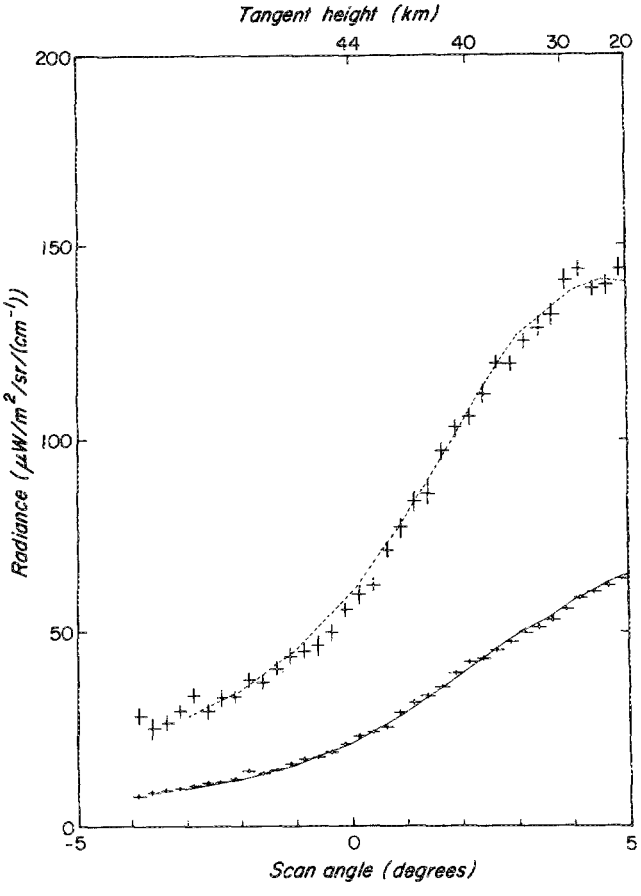

FIG. 11. Signals from the CO channel of the TORBAR instrument at an altitude of 45 km. The signals have been sorted into scan angle bins ($\Delta\theta = 0.25°$) and time averaged over the late morning of August 8th 1985 (3-h time period). The sideband signal (upper) is noisier than the wideband signal (lower) because the spectral bandwidth is narrower. The PMC (path length of 10-mm) pressure varied between 2000 and 800 Pa at a temperature of 273 K.

The equations for the wideband and sideband signals S_w and S_s, respectively, are

$$S_w = G \int_{-\infty}^{\infty} \tau_f \bar{\tau}_p B[\tilde{\nu}, T(x)] \tau_c d\tilde{\nu},$$

$$S_s = G' \int_{-\infty}^{\infty} \tau_f (|\tau_p - \bar{\tau}_p|) B[\tilde{\nu}, T(x)] \tau_c d\tilde{\nu}.$$

G and G' are the combined radiometric and electronic gains of the wideband and sideband signal channels, τ_f is the filter transmission, τ_p is the instantaneous pressure modulator cell transmission, and τ_c is the transmission of the test cell. An overbar indicates a time average. Wave number dependencies in all terms have been dropped for clarity.

In order to concentrate on the gas properties at the expense of the instrumental gains, which are only required to be stable, the ratio S_s/S_w is used, normalized to the empty test cell. This process results in a determination of modulator "transmissions" which can be compared to calculations. In several cases the value of S_w is only slightly influenced by the term involving the test cell, τ_c, and therefore this term can be considered as being a monitor of the source intensity and the ratio as a method of eliminating the effect of source intensity variations from the experiment.

Although for mechanical reasons the test cell used is short, the average pressure and total amount can be made comparable with that of the stratospheric limb path by raising the mixing ratio from a typical stratospheric value of 10^{-8} to about 0.01–0.1. At concentrations higher than this value the correction to the "infinite dilution" solution for the gas becomes appreciable and requires a detailed knowledge of the "self-broadening coefficient" or equivalently the magnitudes of the collision-broadened halfwidths for both self-collisions and collisions with the other gases in the mixture, notably N_2 and O_2. These data are available for some gases, e.g., CO (Ref. 9), but not for all, and may vary considerably from line to line and gas to gas. Thus measurements with pure gas and gas mixtures at various dilutions are required.

The technique we have adopted is to inject a sample of pure gas into the transmission cell and then add inert broadening gas (N_2) to increase the total pressure. We have found that extreme care is required to ensure that the gases are uniformly mixed and that the mixture concentration is known and can be duplicated. In the case of CH_2O, particular care must be taken as the CH_2O in the transmission cell must be generated, thus one must be certain that the CH_2O gas level is stable prior to mixing in N_2.[10,11] Since all the experimental parameters are known, the instrumental results can be compared with the theoretical calculations. We have performed this experiment for both CO and CH_2O using both pure gas and gas/N_2 mixtures.[10,11,12] The results of a single CH_2O/N_2 experiment are shown in Fig. 12.

VII. ATMOSPHERIC MODELLING

The equations that describe the pressure modulator signals from an atmospheric path are

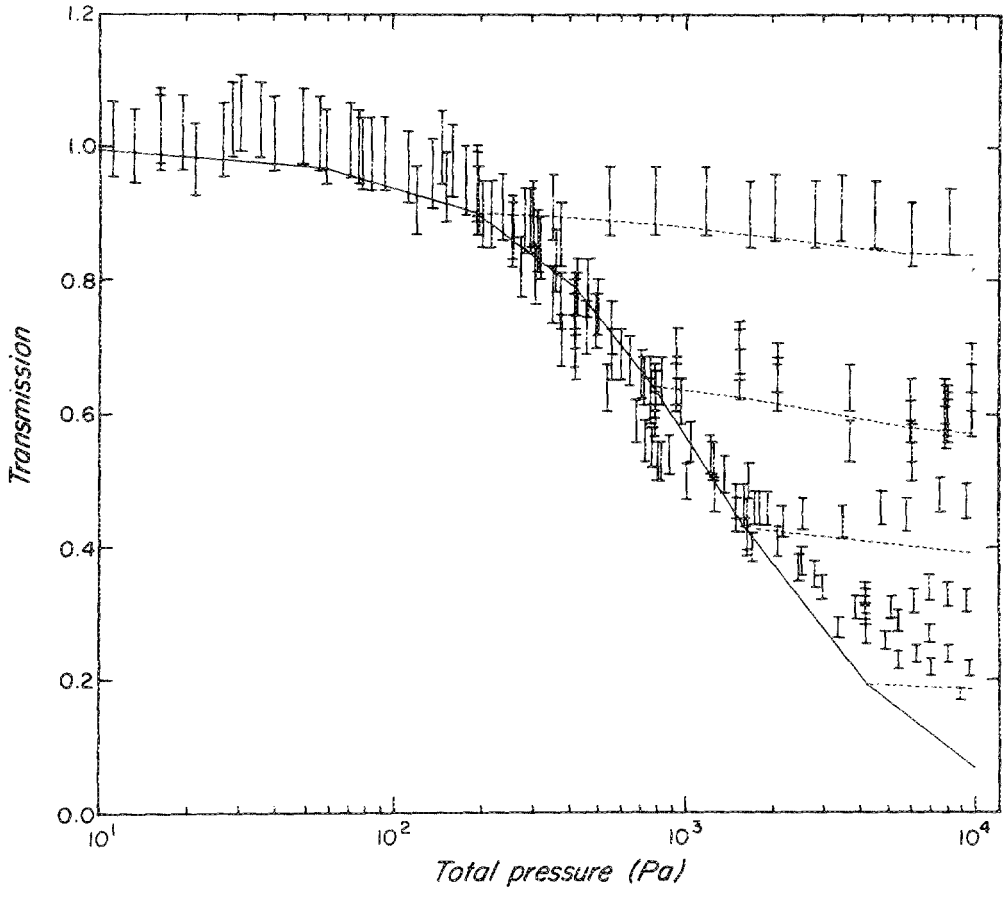

FIG. 12. Comparison of experimental results with GENLEN predictions for a series of CH_2O transmission experiments. The solid line represents pure CH_2O in the transmission cell and the dashed lines represent cases with fixed amounts of CH_2O (190, 780, 1620, and 4220 Pa) mixed with N_2 in the transmission cell. Deviation from the calculations can be seen at high amounts, but these are unrealistic for atmospheric soundings. The PMC operated between 2600 Pa and 500 Pa at a temperature of 298 K. The test cell length is 101 mm and the PMC length is 10 mm.

$$S_w = G \int_{-\infty}^{\infty} \int_0^{\infty} \tau_f \bar{\tau}_p B\,[\tilde{\nu},T(x)]\,\frac{d\tau(0,x)}{dx}\,dx\,d\tilde{\nu}$$

for the wideband signal and

$$S_s = G' \int_{-\infty}^{\infty} \int_0^{\infty} \tau_f(\,\overline{|\tau_p - \bar{\tau}_p|}\,) \times B\,[\tilde{\nu},T(x)]\,\frac{d\tau(0,x)}{dx}\,dx\,d\tilde{\nu}$$

for the sideband signal. B is the Planck function and T the local temperature along the ray path, x, which goes from zero at the instrument to infinity. $\tau(0,x)$ is the atmospheric transmission from the instrument to the point x on the path.

Because of the complexity of the atmospheric situation the models used to evaluate these integrals are also complex, consisting of a multilayer general line-by-line emission model supplemented by simpler models for rough calculations at higher speed. A discussion of the models used is given elsewhere.[13] Each of the spectral regions used has a different set of emitting gases and these influence the relationship between the wideband and sideband signal considerably. In particular, both the CH_2O wideband and sideband channels appear to be strongly influenced by H_2O and O_3 and HNO_3. Their influence is so strong that the CH_2O emissions may be masked by them. The carbon monoxide channels are influenced by ozone. Ozone accounts for all the wideband signal and about 70% of the sideband signal, implying a strong overlap between the ozone and carbon monoxide spectra. In fact, an examination of the spectra reveals an almost exact overlap between the P-branch of the CO spectrum and the 4.8-μm ozone band which consists of a very large number of weak lines. On the other hand, the methane sideband channel appears to be insensitive to the presence of N_2O, whereas the wideband is strongly influenced by N_2O.[13]

VIII. CONCENTRATION PROFILES

The concentration profile of carbon monoxide has been determined for the final phase of the flight of August 8th 1985 which corresponds to late morning. This is shown in Fig. 13. The profile was fitted by first fitting an ozone profile to the wideband signal (the contribution of CO to this signal is negligible), followed by the use of that ozone profile with a CO profile to fit the sideband signal. In both cases a manual iterative scheme was used to match the actual radiance with a computed radiance starting at the top of the atmosphere and working down. The comparison between the final computed radiance and the actual measurements is shown in Fig. 11. Perfect matching is not obtained and a mismatch around the balloon level is exaggerated by the scaling of Fig. 11 in angle. Profiles with a closer match show unreasonable "noise" as large fluctuations in the concentrations with altitude, which is physically difficult to reconcile with the long path length used in limb scanning which has a smoothing effect.

The errors on this profile are difficult to represent because of the interdependence of the radiances from various tangent levels. In order to obtain an estimate of the sensitivity of the profile to errors in the radiance, a "truncated spike" of increased concentration, 3 km thick, was intro-

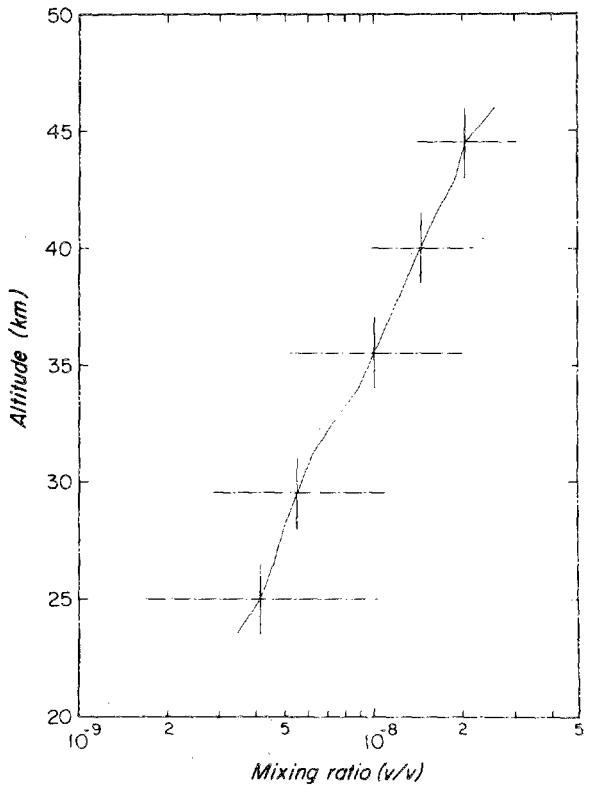

FIG. 13. Carbon monoxide profile for late morning over the southern Canadian prairies on August 8th 1985. The vertical error bar is the mean thickness of a truncated triangular spike used to calculate the horizontal error bars. The horizontal error bars represent the magnitude of the spike required to change the calculated radiance by one standard deviation. Each error bar was derived independently.

duced into the concentration profile. The magnitude of the spike was adjusted so that the calculated radiance changed by approximately one standard deviation of the measured radiances over the relevant portion of the radiance path. The error is substantially influenced by the magnitude of the underlying ozone signal and if this were eliminated, the errors would be considerably less. In future flights, it would be advantageous to select only the CO *R* branch as the elimination of the ozone signal would more than compensate for the loss of 50% of the signal.

Further discussion of the above results and the results from the other channels will be presented elsewhere.[13]

IX. DISCUSSION

The first series of flights of the Toronto Balloon radiometer instrument have provided valuable additional data on the concentration of carbon monoxide and other carbon components in the stratosphere. It is expected that refinements of the instrument will allow the precision of the measurements to be increased and the flexibillty of the instrument will allow it to be rapidly adapted to measure other gases. One such possibility is to equip the instrument to study the time variations of the nitrogen oxides as well as provide a confidence check on the instruments for global measurements of the same gases on the Upper Atmosphere Research Satellite, due for launch in the early 1990s.

ACKNOWLEDGMENTS

The TORBAR project is supported by grants from the National Science and Engineering Research Council of Canada, Atmospheric Environment Service and the Physics Department, University of Toronto. We would like to thank the workshop staff of the Department of Physics for their assistance with the instrument fabrication, the staff of ADGA systems for their support during the flight preparations of this instrument and the staff of the Canada Center for Space Science for their assistance with instrument preparation and funding of the flight itself. The data presented here were gathered during the 1985 balloon campaign with the assistance of S. Heggie and R. Cameron.

[1]F. W. Taylor, *Pressure Modulator Radiometry*, in Vol. III of *Spectroscopic Techniques*, edited G. A. Vanasse (Academic, New York, 1983).
[2]C. P. Chaloner, J. R. Drummond, J. T. Houghton, R. F. Jarnot, and H. K. Roscoe, Proc. R. Soc. London A **364**, 145 (1978).
[3]J. R. Drummond and R. F. Jarnot, Proc. R. Soc. London A **364**, 237 (1978).
[4]J. R. Drummond, J. T. Houghton, G. D. Peskett, C. D. Rodgers, M. J. Wale, J. Whitney, and E. J. Williamson, Phil. Trans. R. Soc. London A **296**, 19 (1980).
[5]J. R. Drummond and A. Ashton, J. Atmos. and Oceanic Tech. (in press).
[6]J. C. Gille and F. B. House, J. Atmos. Sci. **28**, 1427 (1971).
[7]J. R. Drummond, D. Turner, and A. Ashton, J. Atmos. and Oceanic Tech. **3**, 9 (1986).
[8]A. E. Murray, Infrared Physics **2**, 37 (1962).
[9]T. Nakazawa and M. Tanaka, J. Quant. Spectrosc. Radiat. Transfer **28**, 471 (1982).
[10]A. G. Ashton, Stratospheric Measurements of CO Concentration, M.Sc. Thesis (Department of Physics, University of Toronto, 1985).
[11]D. Turner, Radiometric Measurements of CH_2O Concentration, M.Sc. Thesis (Department of Physics, University of Toronto, 1983).
[12]D. Turner, Radiometric Measurements of Stratospheric Trace Gases, Ph.D. Thesis (Department of Physics, University of Toronto, 1987).
[13]D. Turner and J. R. Drummond (unpublished).